

## Effect of Temperature on the Dielectric Properties of CoFe<sub>2</sub>O<sub>4</sub> Ferrite

V.S. Bushkova\*, B.K. Ostafiychuk, T.O. Semko

Vasyl Stefanyk Pre-Carpathian National University, 57, Shevchenko St., 76025 Ivano-Frankivsk, Ukraine

(Received 30 August 2016; published online 23 December 2016)

The temperature-frequency dependences of the dielectric constants of cobalt ferrite prepared by sol-gel method involving auto-combustion was studied in the work by impedance spectroscopy. It was established that the course of the curves presented in Nyquist coordinates depends on temperature. With increasing frequency, the real  $\epsilon'$  and imaginary  $\epsilon''$  components of the dielectric permittivity decrease due to the mechanism of the polarization process that is typical for ferrites. In the frequency dependence of the tangent of the dielectric loss angle  $\text{tg}\delta$ , it was found the maximum at a temperature of 298 K at  $f = 56$  Hz, since for this frequency, the carrier jump frequency coincides with the frequency of the applied external field. It is shown that with increasing temperature, the specific conductivity of ferrite CoFe<sub>2</sub>O<sub>4</sub> also increases. The dependence  $\sigma(f)$  indicates the existence in the studied sample of the DC conductivity, the contribution of which into the dielectric response significantly increases with temperature. It is established that the activation energy of carriers  $\Delta E_A$  is equal to 0.49 eV.

Keywords: Sol-gel method, Cobalt ferrite, Impedance spectroscopy, Dielectric permittivity, Specific conductivity, Activation energy.

DOI: [10.21272/jnep.8\(4\(2\)\).04069](https://doi.org/10.21272/jnep.8(4(2)).04069)

PACS numbers: 75.50.Tt, 43.58.Bh, 77.22. – d, 72.80.Le

### 1. INTRODUCTION

By the response to an external magnetic field and by the internal magnetic ordering all substances in nature can be divided into five groups [1], such as diamagnets, paramagnets, ferromagnets, antiferromagnets and ferrimagnets. Five different types of magnetic states of matter correspond to the above types of magnetic materials: diamagnetism, paramagnetism, ferromagnetism, antiferromagnetism and ferrimagnetism.

Ferrimagnets include substances, the magnetic properties of which are due to uncompensated antiferromagnetism. Thus, like ferromagnets, they have high magnetic susceptibility, which essentially depends on the magnetic field strength and temperature. At the same time, ferrimagnets are also characterized by a number of significant differences from ferromagnetic materials. Some ordered metal alloys have ferrimagnetic properties, but, mainly, these are various oxide compounds, among which ferrites are of the greatest practical interest [2].

Modern communication devices use many parts with ferrite cores [3, 4]. Ferrites satisfy rigorous requirements for modern elements of communication devices, as well as find other applications [5-7]. These are, for example, ferrite antennas, unidirectional waveguide isolators, microwave modulators. The production of ferrites of various compositions increases the possibilities of their use, thereby ferrites exceed the application limits, for which they were originally developed, and began to be used in computer technology, measurement control techniques and atomic technology.

Cobalt ferrite is known as a hard magnetic material with high coercivity and low magnetization. These properties, along with high physical and chemical stability, facilitate its use in data storage devices, as well as in magneto-optical and magneto-electric devices [8-11].

This work is devoted to the study of the temperature-frequency dependences of the dielectric properties of the CoFe<sub>2</sub>O<sub>4</sub> ferrite obtained by the sol-gel auto-combustion (SGA) method [12].

### 2. EXPERIMENTAL

CoFe<sub>2</sub>O<sub>4</sub> ferrite powder was obtained using the SGA method. The phase composition was controlled by X-ray analysis, which was performed using a DRON-3 diffractometer with Cu( $K\alpha$ ) radiation in the range of scan angles of  $20^\circ \leq 2\theta \leq 60^\circ$  and with a step of  $0.02^\circ$ . According to the conducted analysis, the peaks of the XRD patterns indicate the presence of the spinel cubic structure of the  $Fd\bar{3}m$  space group [13].

A ferrite brick with a diameter of 0.8 cm and a height of 0.12 cm was obtained by pressing at 30 kN a synthesized powder with the addition of a binder, namely, 10 % solution of polyvinyl alcohol. This sample was subjected to sintering at a temperature of 1300 °C for 5 hours in an atmosphere of air with slow cooling. After sintering and grinding, a cobalt ferrite brick with the following geometry was obtained: diameter 0.68 cm and height 0.1 cm. Thus, the linear seal of the sample  $\Delta L/L$  was 0.15.

A graphite electrode/ferrite brick/graphite electrode capacitor system was fabricated to carry out impedance studies. The dielectric and conducting characteristics of the investigated ferrite sample were determined by the parameters of the complex impedance

$$Z = Z' - jZ'' \quad (1)$$

(here  $Z'$  and  $Z''$  are the real and imaginary parts of the complex impedance,  $j$  is the imaginary unit), the measurements of which were carried out using the PGSTAT 12/FRA-2 Autolab spectrometer in the frequency range of  $10^{-2}$ - $10^6$  Hz. The temperature measurements were conducted in the range from 298 K to 723 K with a step of 25 K using an SNOL 7.2/1100 electric furnace.

Taking into account the sample geometry, the specific resistivities and frequency dependence of the electrical parameters were calculated

$$\rho = \rho' - j\rho'' \quad (2)$$

$$\rho' = \frac{S}{h} Z', \quad \rho'' = \frac{S}{h} Z'' \quad (3)$$

\* [bushkovavira@gmail.com](mailto:bushkovavira@gmail.com)

where  $S$  and  $h$  are the sample base area and height, respectively.

The complex specific conductivity was determined by the following relationship:

$$\sigma = \frac{1}{\rho} = \sigma' + j\sigma'' \tag{4}$$

$$\sigma' = \frac{\rho'}{M}, \quad \sigma'' = \frac{\rho''}{M} \tag{5}$$

$$M = \left(\frac{S}{h}\right)^2 \cdot |Z|^2 \tag{6}$$

Similarly, based on the measured values of  $Z'$ ,  $Z''$ , the real and imaginary components of the complex dielectric permittivity were determined using the correlations

$$\varepsilon = \varepsilon' - j\varepsilon'' \tag{7}$$

$$\varepsilon' = \frac{\rho''}{M\omega\varepsilon_0} = \frac{h}{S|Z|^2\omega\varepsilon_0} \cdot Z'' \tag{8}$$

$$\varepsilon'' = \frac{\rho'}{M\omega\varepsilon_0} = \frac{h}{S|Z|^2\omega\varepsilon_0} \cdot Z' \tag{9}$$

where  $\omega = 2\pi f$ ,  $\varepsilon_0$  is the permittivity of vacuum.

The dielectric losses are calculated by the formula

$$\text{tg}\delta = \frac{\varepsilon''}{\varepsilon'} \tag{10}$$

### 3. RESULTS AND DISCUSSION

#### 3.1 Temperature characteristic of the impedance hodograph curves

Fig. 1 presents the impedance hodographs  $Z'' = f(Z')$ . The nature of the curves presented in Nyquist coordinates depends on temperature. For example, dependences  $Z''(Z')$  in the temperature range of 298-373 K represent a loop consisting of two semicircles. The first area is responsible for the contribution to the dielectric response of the sample grain volume. The presence of the second area located to the right of the previous one, can be associated with the contribution to the dielectric response of grain boundaries or other electrical barriers [14].

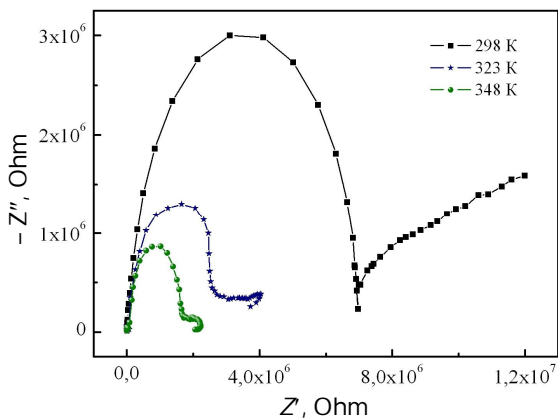


Fig. 1 – Temperature dependences of  $\text{CoFe}_2\text{O}_4$  impedance hodographs

With increasing temperature, the second area in the Nyquist diagram narrows and completely disappears at a temperature of 398 K (see Fig. 2).

A similar behavior of the dependence  $Z''(Z')$  is observed up to  $T = 448$  K inclusive. Already at a temperature of  $\geq 473$  K, the Nyquist diagram (see Fig. 3) changes its shape and looks like an acute angle, which is about  $45^\circ$ , and at a temperature of  $\geq 673$  K, the dependence  $Z''(Z')$  represents a curve which approaches in shape the right angle (Fig. 4).

The analysis of the diagrams  $Z''(Z')$  showed that the value of the cobalt ferrite resistance significantly decreases with increasing temperature that, in fact, is typical for semiconductors.

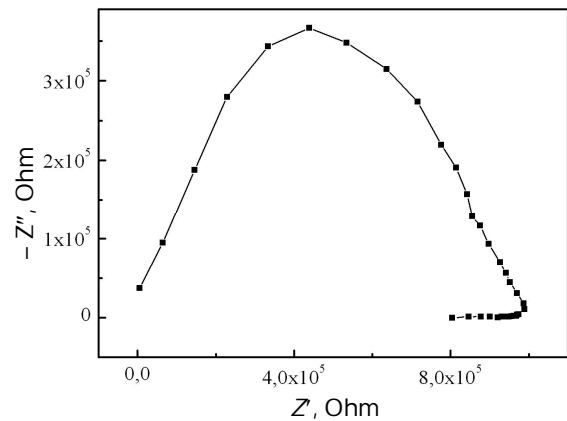


Fig. 2 – Nyquist diagram at a temperature of 398 K

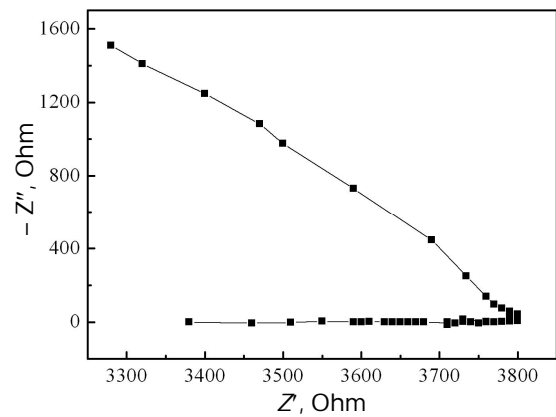


Fig. 3 – Dependence  $Z''(Z')$  at a temperature of 548 K

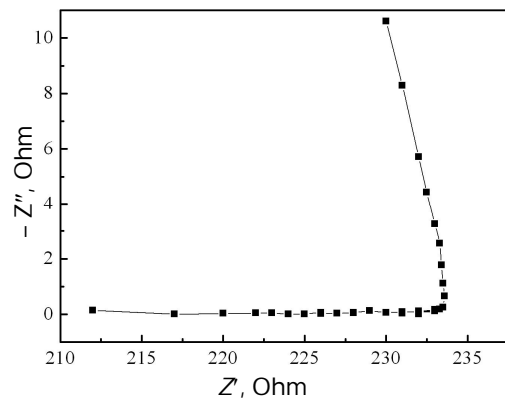


Fig. 4 – Frequency impedance spectrum at a temperature of 698 K

### 3.2 Dielectric losses in cobalt ferrite

In Fig. 5 we illustrate the frequency dependences of the real  $\epsilon'$  and imaginary  $\epsilon''$  parts of the complex permittivity at a temperature of 298 K. The main trend is that the values of  $\epsilon'$  and  $\epsilon''$  decrease with increasing frequency for all temperatures.

This behavior of the real and imaginary parts of the complex permittivity is explained by the mechanism of the polarization process in ferrites. Due to electronic exchange  $\text{Fe}^{2+} \leftrightarrow \text{Fe}^{3+} + e^-$ , there is a local displacement of electron that influences the polarization in ferrites [15] along the applied electric field direction. With increasing frequency, the polarization decreases as a result of the fact that at a certain electric field frequency, there is no electronic exchange between the  $\text{Fe}^{2+}$  and  $\text{Fe}^{3+}$  ions due to the applied field action.

As clearly seen from Fig. 5, the tangent of the dielectric loss angle  $\text{tg}\delta < 1$  at  $f > 1.67$  kHz. It should be noted that this frequency increases with increasing temperature. Thus, for example, at a temperature of 323 K, this frequency is 5.25 kHz, and for  $T = 348$  K – 7.54 kHz. Therefore, cobalt ferrite can compete by the parameter  $\text{tg}\delta$  with ordinary dielectrics at frequencies higher than  $10^3$  Hz.

In Fig. 6 we present the frequency dependence of the tangent of the dielectric loss angle at a temperature of 298 K. As seen from the figure, a sharp maximum, the value of which is equal to 30, is observed at  $f = 56$  Hz.

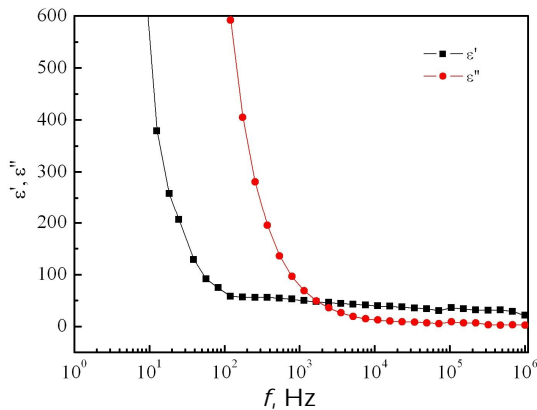


Fig. 5 – Dependence of the real  $\epsilon'$  and imaginary  $\epsilon''$  parts of the complex dielectric permittivity for different frequencies

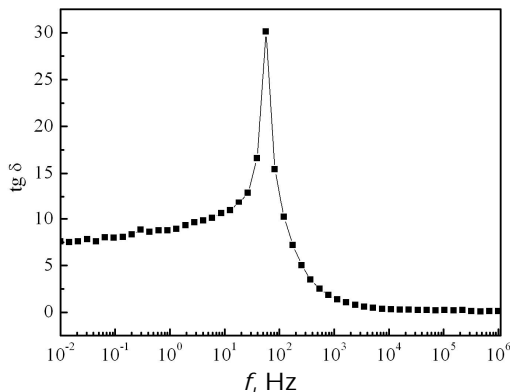


Fig. 6 – Frequency dependence of the loss tangent

Fig. 7 presents the frequency dependence of the loss tangent for different temperatures. As seen from Fig. 7, a general tendency to decrease the dielectric losses with increasing frequency is observed for the indicated temperatures. At the same time, it should be noted that at a temperature of 323 K for  $f = 56$  Hz, there is a peak in the figure, which is weaker in intensity and equals 26. Along with this, at  $T = 348$  K, besides the peak at the above frequency, there is another one at a frequency of 255 Hz, which is much more intense at 373 K. However, at  $T \geq 398$  K, the peak at a frequency of 56 Hz completely disappears, and the second peak intensity increases with increasing temperature at which sample  $\text{CoFe}_2\text{O}_4$  is studied (Fig. 8). The reason for this dependence of the loss tangent can be the following: with increasing temperature, the maximum at a frequency of 255 Hz appears due to the probable activation of the fault motion at the grain boundaries towards the surface that is a manifestation of intergranular polarization.

The authors of [16] also detected a peak for lithium magnesium ferrites in the range of 50 Hz at room temperature. As known [17], largely, the maximum in the frequency dependence of the loss tangent arises in that case, when the carrier jump frequency coincides with the frequency of the applied external field.

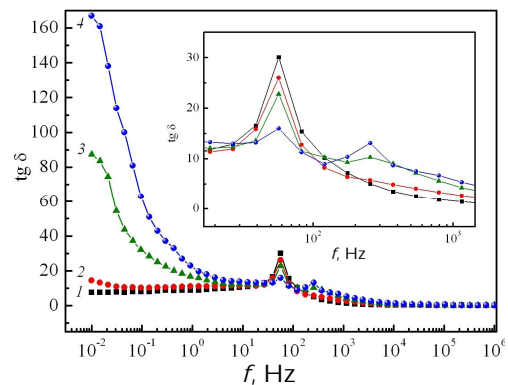


Fig. 7 – Frequency dependence of  $\text{tg}\delta$ : 1 – 298 K, 2 – 323 K, 3 – 348 K, 4 – 373 K

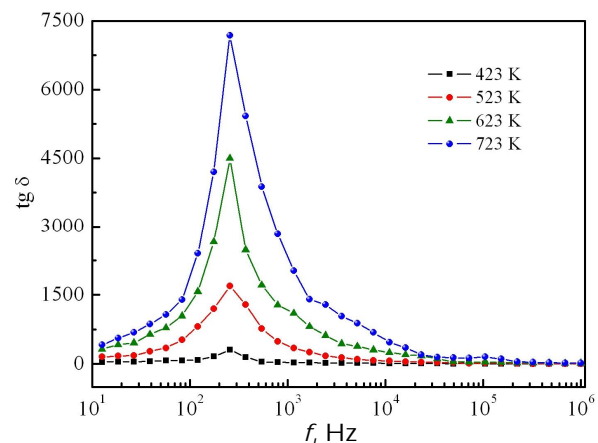


Fig. 8 – Tangent of the dielectric loss angle as a function of frequency at different temperatures

### 3.3 Study of the dielectric permittivity of CoFe<sub>2</sub>O<sub>4</sub> depending on temperature

A relatively high dielectric permittivity, which depends on the frequency, temperature and, above all, the material composition is typical for ferrites. With increasing frequency, as a rule, the dielectric permittivity of ferrites decreases. Thus, for example, at room temperature, the real part of the relative dielectric permittivity of cobalt ferrite at a frequency of 10 Hz is 550 and at  $f = 10^2$  Hz it is equal to 66, and at  $f = 10^3$  Hz – 40.

The experimental data on the change in the real part of the dielectric permittivity with temperature at different frequencies are shown in Fig. 9. For all frequencies,  $\epsilon'$  monotonously increases with increasing temperature in the temperature range of 298-623 K; however, there is a sharp increase in the dielectric permittivity in the temperature range of 623-698 K. The curve  $\epsilon'(T)$  has a maximum on a frequency of  $10^{-2}$  Hz at a temperature of 673 K, and on a frequency of  $10^6$  Hz – at  $T = 698$  K. Thus, the change in the real part of the dielectric permittivity with temperature has a maximum in the high-temperature region, which shifts to higher temperatures with increasing frequency. Ions of variable valence have a great influence on the polarization properties of ferrites. An increase in the material dielectric permittivity is usually observed with increasing their concentration.

As known [18, 19], in polycrystalline ferrites, the dielectric conductivity, as well as the specific conductivity, depends on the structure, for example, on the grain size of the sample, which, in turn, depends on the synthesis method and the ferrite composition. Unlike grains, their boundaries have a higher concentration of vacancies and other inhomogeneities that mostly affects the electrophysical properties of ferrites. The more ionic vacancies and weakly bound electrons are in ferrites, the greater the number of dipoles they form, and the higher the dielectric permittivity will be. Obviously, the optimum temperature for the formation of such dipoles at grain boundaries is in the range of 673-698 K depending on the frequency, which results in a sharp increase in the real part of the dielectric permittivity of cobalt ferrite.

In Fig. 10 we present the temperature dependence of the imaginary part of the dielectric permittivity. As seen, they are described by smooth curves, the course of which depends on frequency. A sharp increase in  $\epsilon''$  is observed at low frequencies.

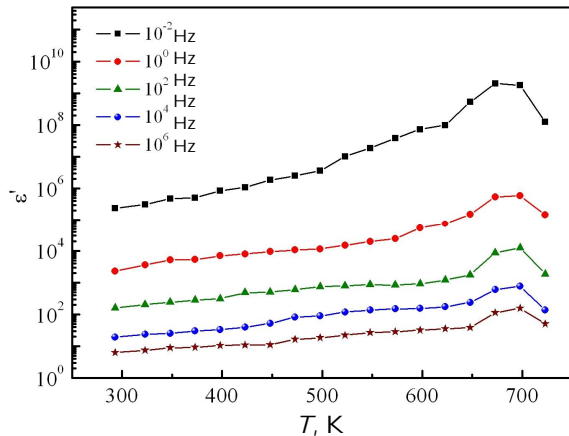


Fig. 9 – Temperature dependence of the real part of the dielectric permittivity for different frequencies

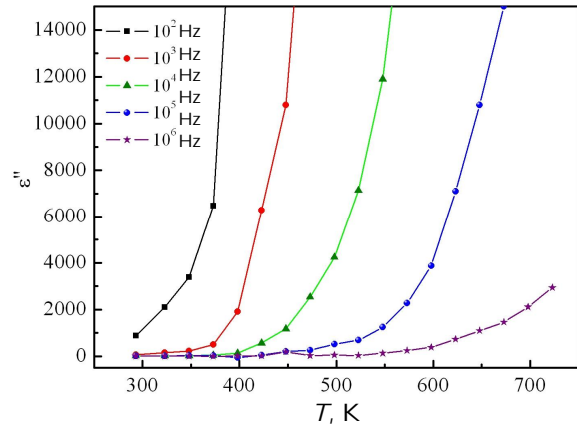


Fig. 10 – Temperature dependence of the imaginary part of the dielectric permittivity for different frequencies

Such a frequency dependence of  $\epsilon''$  is a consequence of grain boundary polarization, which is based on the 2-layer Maxwell-Wagner model. The grain-boundary polarization occurs because of the structural inhomogeneity in ferrites. Due to the existence of free charges, the electrons jumping at low frequencies can be trapped by inhomogeneities [20], which prevent the free transfer of electric charges in the sample resulting in the accumulation of the latter in some identified its regions. An increase in  $\epsilon''$  with increasing temperature at a certain frequency is a consequence of a decrease in the resistance of ferrites. Because of the low resistance facilitating to the electronic transitions, a higher polarization is observed, that is, the value of  $\epsilon''$  increases.

### 3.4 Temperature dependence of the specific conductivity of ferrites

According to the electrical properties, ferrites belong to semiconductors. Their electrical conductivity is due to the electron exchange processes between ions of variable valence. The electrons participating in the exchange can be considered as charge carriers, whose concentration is almost temperature-independent. At the same time, with increasing temperature, the probability of electron jump between ions of variable valence exponentially increases, that is, the charge carrier mobility increases. Therefore, the temperature change in the specific conductivity of ferrites with sufficient (for practical purposes) accuracy can be described by the following formula:

$$\sigma = \sigma_0 \exp\left(-\frac{\Delta E_A}{kT}\right), \quad (11)$$

where  $\sigma_0$  is the pre-exponential factor, which does not depend on temperature,  $\Delta E_A$  is the activation energy of DC carriers,  $k$  is the Boltzmann constant.

In Fig. 11a we illustrate the frequency dependence of the real part of the specific conductivity in logarithmic coordinates. The dependence  $\sigma'(f)$  begins to increase at room temperature for  $f > 10^3$  Hz. Deviation from linearity of the frequency dependence of the real part of the electrical conductivity is observed for  $T \leq 523$  K, at that the frequency of deviation from linearity increases with increasing temperature; and for  $T \geq 548$  K (Fig. 11b) the above dependence reaches a plateau. This indicates that in the studied ferrite, there is the DC conductivity,

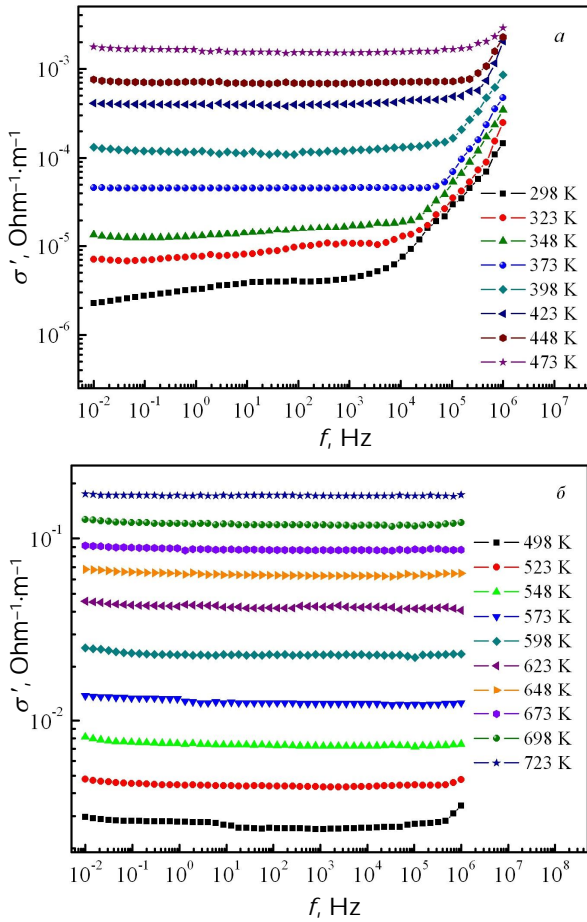


Fig. 11 – Frequency dependence of the real component of the specific conductivity of cobalt ferrite at different temperatures: a –  $T \leq 473$  K, b –  $T \geq 498$  K

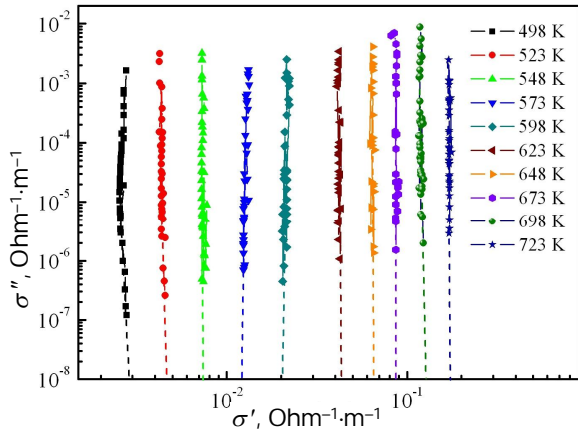


Fig. 12 – Diagrams  $\sigma''(\sigma')$  at  $T \geq 498$  K

whose contribution to the dielectric response increases with temperature and becomes dominant at  $T \geq 548$  K.

The frequency dependence of the real component of the specific electrical conductivity is described by the Debye relaxation formula

$$\sigma = \sigma_{dc} + A\omega^n, \tag{12}$$

where  $A$  and  $n$  are the parameters, which depend on the temperature and composition. The term  $A\omega^n$  is responsible for the polarization component of the specific conductivity. The proportionality factor  $A$  is determined as

$$A = \frac{nq^2\delta^2v}{6k}, \tag{13}$$

where  $v$  is the oscillation frequency of ions in the lattice sites,  $n$ ,  $q$ ,  $\delta$  are, respectively, the concentration, charge, and carrier free path, and  $k$  is the Boltzmann constant.

The value of  $\sigma_{dc}$  for  $\text{CoFe}_2\text{O}_4$  at various temperatures is estimated using the diagrams  $\sigma''(\sigma')$  by extrapolating the relationships between  $\sigma''$  and  $\sigma'$ , which in the low-frequencies range have the form of straight line segments, to the intersection with the abscissa (Fig. 12).

### 3.5 Determination of the carrier activation energy

Among the many factors influencing the electrical resistance of ferrites, the concentration of divalent iron ions  $\text{Fe}^{2+}$  is the main one. Under the effect of thermal motion, the weakly bound electrons jump from iron ions  $\text{Fe}^{2+}$  to ions  $\text{Fe}^{3+}$  and reduce the valence of the latter. With increasing concentration of divalent iron ions, the material conductivity linearly increases and the activation energy  $\Delta E_A$  decreases simultaneously. The hole exchange between  $\text{Co}^{2+}$  and  $\text{Co}^{3+}$  ions is also possible for cobalt ferrite [21]. It follows that with approaching ions of variable valence, there is a decrease in the height of energy barriers, which should be overcome by electrons when passing from one ion to the neighboring. In spinel ferrites, the activation energy of electrical conductivity is usually in the range from 0.1 to 0.5 eV. Magnetite  $\text{Fe}_3\text{O}_4$  with  $\rho = 5 \cdot 10^{-5} \text{ Ohm}\cdot\text{m}$  has the highest concentration of divalent iron ions and, correspondingly, the smallest resistivity [22].

In Fig. 13 we show the dependence of  $\ln(\sigma_{dc})$  on the inverse temperature. It is seen from the figure that the above dependence is linear in the Arrhenius coordinates. The presence of a straight line region in the temperature dependence of the specific conductivity represented in the coordinates of  $\ln(\sigma_{dc})$  on  $10^3/T$  indicates the realization of the electrical conductivity activation mechanism.

The activation energy is calculated by the formula

$$\Delta E_A = \frac{kT_1T_2}{T_1 - T_2} \cdot \ln \frac{\sigma_1}{\sigma_2}, \tag{14}$$

where  $T_1 = 723$  K,  $T_2 = 298$  K,  $\sigma_1$ ,  $\sigma_2$  are the DC specific conductivities corresponding to the stated temperatures.

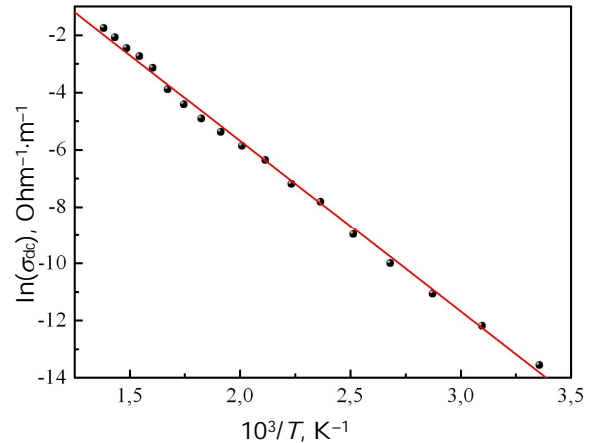


Fig. 13 – Dependence of the logarithm of the DC specific conductivity on the inverse temperature

## 4. CONCLUSIONS

Thus, the study of the dielectric characteristics found from the analysis of the impedance spectra at different temperatures allowed to reveal the regularities of their change depending on frequency. Based on the Nyquist diagrams, the resistance of cobalt ferrite significantly decreases with increasing temperature.

The temperature dependence of the dielectric characteristics of cobalt ferrite is associated with the process of thermal excitation of charge carriers. Thus, the electron exchange between  $\text{Fe}^{2+}$  and  $\text{Fe}^{3+}$  ions affects the polarization in  $\text{CoFe}_2\text{O}_4$  ferrite. In addition, the nonmonotonic nature of the temperature dependence of the real part of

the dielectric permittivity implies the existence of a contribution to the polarization of the grain boundary processes, which is manifested in the vicinity of temperatures of 673-698 K.

A typical increase in  $\text{tg}\delta$  with decreasing frequency is a sign of the presence of the DC electrical conductivity. Based on the diagrams  $\sigma''(\sigma')$ , we estimated the value of  $\sigma_{dc}$  as a function of temperature, the behavior of which is well described by the exponential law, that is the DC electrical conductivity expectedly increases with increasing temperature. According to the measurement results of the DC conductivity of  $\text{CoFe}_2\text{O}_4$  spinel, the activation energy of charge carriers, which is equal to 0.49 eV for the studied temperature range, is determined.

## REFERENCES

1. V.A. Bokov, *Fizika magnitnykh materialov* (Sankt-Peterburg: Nevskiy dialekt: 2002).
2. Y.H. Hou, Y.J. Zhao, Z.W. Liu, H.Y. Yu, X.C. Zhong, W.Q. Qiu, D.C. Zeng, L.S. Wen, *J. Phys. D: Appl. Phys.* **43**, 44 (2010).
3. S. Krupichka, *Fizika ferritov i rodstvennykh im materialov* (Moskva: Mir: 1976).
4. P. Zbigniew, *J. Eur. Ceramic Soc.* **24**, 1053 (2004).
5. Q. Song, Z.J. Zhang, *J. Am. Chem. Soc.* **126**, 6164 (2004).
6. M.A. Ahmed, N. Okasha, L. Salah, *J. Magn. Magn. Mater.* **264**, 241 (2003).
7. X. Cao, L. Gu, *Adv. Nan. Phy.* **16**, 180 (2005).
8. J. Ding, Y.J. Chen, Y. Shi, S. Wang, *Appl. Phys. Lett.* **77**, 6398 (1995).
9. Y. Suzuki, R.B. Van Dover, E.M. Gyorgy, J.M. Philips, V. Korenivski, D.J. Werder, C.H. Chen, R.J. Cava, J.J. Krajewski, W.F. Peck, K.B. Do, *Appl. Phys. Lett.* **68**, 714 (1996).
10. J. Ding, T. Reynold, W.F. Miao, P.G. McCormick, R. Street, *Appl. Phys. Lett.* **65**, 7074 (1994).
11. B. Zhou, Y.W. Zhang, Y.J. Yu, C.S. Liao, C.H. Yan, L.Y. Chen, S.Y. Wang, *Phys. Rev. B* **68**, No 22 24426 (2003).
12. V.S. Bushkova, *J. Nano-Electron. Phys.* **7**, No 1 01023 (2015).
13. V.S. Bushkova, *J. Nano-Electron. Phys.* **7**, No 3 03021 (2015).
14. N.M. Olegovich, I.I. Moroz, A.V. Pushkarev, Yu.V. Radish, A.N. Salak, *Phys. Solid State* **50**, 472 (2008).
15. M.A. Ahmed, Samiha T. Bishay, *J. Phys. D: Appl. Phys.* **34**, 1339 (2001).
16. B.K. Ostafiychuk, I.M. Hasyuk, L.S. Kaykan, V.V. Uhorchuk, P.P. Yakubovs'kyi, V.A. Tsap, Yu.S. Kaykan, *Metallofiz. Noveyshie Tekhnol.* **36** No 1 89 (2014).
17. A.V. Malyshev, V.V. Peshev, A.M. Pritulov, *Izv. vuzov. Fizika* No 7, 48 (2003).
18. M.N. Abdullah, A.N. Yusoff, *J. Alloys Compd.* **233**, 129 (1996).
19. M.N. Abdullah, A.N. Yusoff, *J. Mater. Sci.* **32**, 5817 (1997).
20. M.P. Bogdanovich, V.N. Varskoy, V.P. Lebedev, *Izv. vuzov. Fizika* No 1, 58 (1983).
21. Hasan Mehmood Khan, Misbah-ul-Islam, Irshad Ali, Mazhar-ud-din Rana, *Mater. Sci. Appl.* **2**, 1083 (2011).
22. D. Tripathy, A.O. Adeyeye, *J. Appl. Phys.* **103**, 07F701 (2008).
23. Z.Ž. Lazarević, Č. Jovalekić, D. Sekulić, M. Slankamenac, M. Romčević, A. Milutinović, N.Ž. Romčević, *Sci. Sintering* **44**, 331 (2012).
24. S. Balaji, R. Kalai Selvan, L. John Berchmans, S. Angappan, K. Subramanian, C.O. Augustin, *Mater. Sci. Engin. B* **119**, 119 (2005).